# Single-layer MoS2 electronics. — **Source link** ⬈

Dominik Lembke, Simone Bertolazzi, Andras Kis

**Institutions:** École Polytechnique Fédérale de Lausanne

**Published on:** 02 Jan 2015 - Accounts of Chemical Research (American Chemical Society)

**Topics:** Graphene

Related papers:

- Single-layer MoS2 transistors

- Electronics and optoelectronics of two-dimensional transition metal dichalcogenides.

- Atomically thin MoS2: a new direct-gap semiconductor

- Emerging Photoluminescence in Monolayer MoS2

- The chemistry of two-dimensional layered transition metal dichalcogenide nanosheets

# Single-Layer MoS2 Electronics

*Published as part of the Accounts of Chemical Research special issue "2D Nanomaterials beyond Graphene".*

Dominik Lembke, Simone Bertolazzi, and Andras Kis*

Electrical Engineering Institute, École Polytechnique Fédérale de Lausanne (EPFL), CH-1015 Lausanne, Switzerland

**CONSPECTUS:** Atomic crystals of two-dimensional materials consisting of single sheets extracted from layered materials are gaining increasing attention. The most well-known material from this group is graphene, a single layer of graphite that can be extracted from the bulk material or grown on a suitable substrate. Its discovery has given rise to intense research effort culminating in the 2010 Nobel Prize in physics awarded to Andre Geim and Konstantin Novoselov. Graphene however represents only the proverbial tip of the iceberg, and increasing attention of researchers is now turning towards the veritable zoo of so-called "other 2D materials". They have properties complementary to graphene, which in its pristine form lacks a bandgap: $MoS_2$, for example, is a semiconductor, while $NbSe_2$ is a superconductor. They could hold the key to important practical applications and new scientific discoveries in the two-dimensional limit. This family of materials has been studied since the 1960s, but most of the research focused on their tribological applications: $MoS_2$ is best known today as a high-performance dry lubricant for ultrahigh-vacuum applications and in car engines. The realization that single layers of $MoS_2$ and related materials could also be used in functional electronic devices where they could offer advantages compared with silicon or graphene created a renewed interest in these materials. $MoS_2$ is currently gaining the most attention because the material is easily available in the form of a mineral, molybdenite, but other 2D transition metal dichalcogenide (TMD) semiconductors are expected to have qualitatively similar properties.

In this Account, we describe recent progress in the area of single-layer $MoS_2$-based devices for electronic circuits. We will start with $MoS_2$ transistors, which showed for the first time that devices based on $MoS_2$ and related TMDs could have electrical properties on the same level as other, more established semiconducting materials. This allowed rapid progress in this area and was followed by demonstrations of basic digital circuits and transistors operating in the technologically relevant gigahertz range of frequencies, showing that the mobility of $MoS_2$ and TMD materials is sufficiently high to allow device operation at such high frequencies.

Monolayer $MoS_2$ and other TMDs are also direct band gap semiconductors making them interesting for realizing optoelectronic devices. These range from simple phototransistors showing high sensitivity and low noise, to light emitting diodes and solar cells. All the electronic and optoelectronic properties of $MoS_2$ and TMDs are accompanied by interesting mechanical properties with monolayer $MoS_2$ being as stiff as steel and 30× stronger. This makes it especially interesting in the context of flexible electronics where it could combine the high degree of mechanical flexibility commonly associated with organic semiconductors with high levels of electrical performance. All these results show that $MoS_2$ and TMDs are promising materials for electronic and optoelectronic applications.
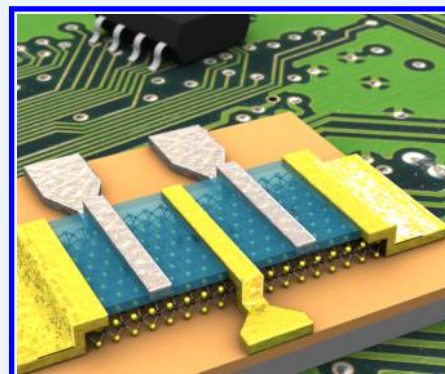
## ■ INTRODUCTION

The most important basic building block of modern electronic circuits is the field-effect transistor (FET), mostly used as a switch in digital circuits. A typical FET is composed of source and drain regions that serve as contacts for the thin area connecting them, the channel. It is covered with a thin dielectric material, the gate dielectric, and capped with a metal electrode, the top gate. This electrode is used to electrostatically control the conductivity of the channel by changing the charge carrier concentration. If the transistor is to be used as a switch, the conductivity should be changed using the gate electrode from a value with high resistance, corresponding to the open position of the switch and called the off state, to a highly conductive on state, corresponding to the closed position of the switch. An ideal switch should also be able to instantly switch between the on and off states.

A good transistor channel material should satisfy several criteria. A material with high charge carrier mobility will allow fast operation and high on state current. Even though important, the mobility is not the only essential material property for transistors, as can be seen in the case of graphene with a high intrinsic mobility but no bandgap, resulting in transistors that cannot be turned off. In order to achieve high on/off ratios, a material with a bandgap is needed, with higher
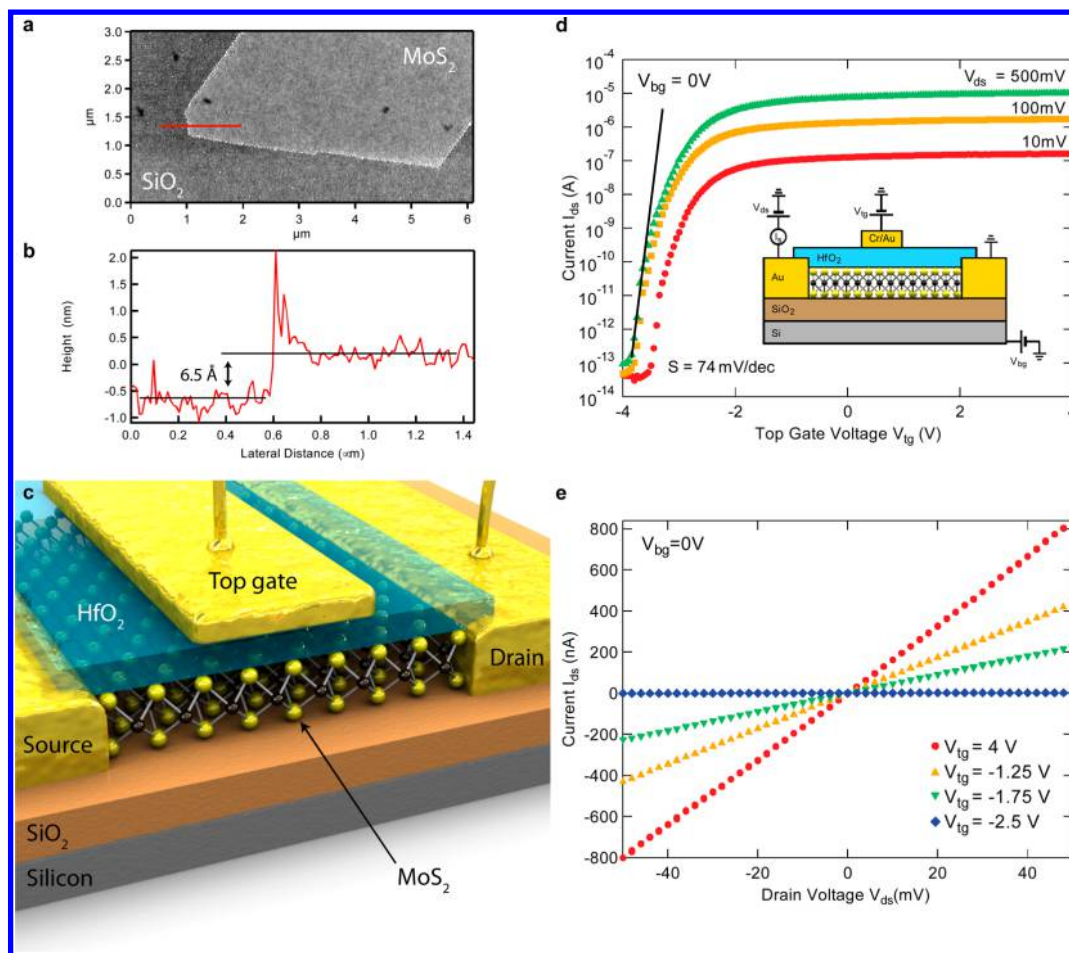
**Figure 1.** Encapsulated single-layer MoS$_2$ transistor. (a) AFM image of single-layer MoS$_2$.[7] (b) Corresponding height profile. (c) Schematic view of the transistor demonstrated by Radisavljevic et al.[8] The MoS$_2$ layer is connected by Au leads and encapsulated in 30 nm thick high-$\kappa$ dielectric HfO$_2$ acting as top-gate dielectric. (d) Transfer curves acquired at room temperature. For $V_{ds}$ = 500 mV, the on/off ratio is >10$^8$ and the subthreshold swing $S$ = 74 mV/dec. Inset: Cross-sectional view of MoS$_2$ FET. (e) Output curves recorded for different top-gate voltages $V_{tg}$. Panels a, b, d, and e adapted from ref 8 with permission. Copyright 2011 NPG. Panel c adapted from ref 42 with permission. Copyright 2011 NPG.

bandgaps resulting in lower off state currents. This is however limited by the fact that materials with higher bandgaps show lower conductivity because of smaller charge carrier concentration. The mobility and bandgap in general also follow an empiric relationship with the mobility decreasing as the bandgap is increased.[1] In order to achieve a sharp switching characteristic (subthreshold swing), a material that allows a high degree of electrostatic control is needed.

As the size of transistors is decreased, the subthreshold swing increases, causing an increase in the off state current. The undesired change in the distribution of electric fields causes short channel effects and can be modeled using the Poisson equation,[2] resulting in a natural length $\lambda$ defined as

$$\lambda = \sqrt{\frac{\varepsilon_{ch}}{N\varepsilon_{ox}}d_{ch}d_{ox}} \tag{1}$$

where $\varepsilon_{ch}$ and $\varepsilon_{ox}$ are dielectric constants of the channel and the oxide and $d_{ch}$ and $d_{ox}$ are the thicknesses of the semiconducting channel and the oxide. $N$ is the effective gate number, equal to 1 for a single gate, 2 for a dual-gate geometry where the semiconducting channel is sandwiched between a pair of gate electrodes, and 3 for a trigate device where the gate surrounds

the channel from three sides. A device can be considered free of short-channel effects if the gate is at least six times longer than $\lambda$.

The natural length can be decreased by decreasing the gate oxide thickness, increasing the gate oxide dielectric constant, and also modifying the channel material and replacing it with a thinner layer that also has a lower dielectric constant. Two-dimensional materials that represent the ultimate limit of miniaturization in the vertical dimension are therefore very interesting in this context because they would allow a very high degree of electrostatic control. One such example is transition metal dichalcogenides (TMDs), with single-layer MoS$_2$ being the typical representative of semiconducting TMDs.[3]

Even though some of the semiconducting properties of TMDs have been known for decades, with reports of successful exfoliation of thin-film MoS$_2$ published by Frindt et al. in 1963,[4] they have not been seriously considered for applications in semiconductor electronics until recently. Some of the first electrical measurements on semiconducting TMDs date back to the 1960s, when Fivaz and Moser showed that the carrier mobility of MoS$_2$, MoSe$_2$, and WSe$_2$ exceed 100 cm$^2$/(V s) in the direction along the layers.[5] In 2004, the first transistors were fabricated on the surface of bulk WSe$_2$ crystals,[6] showing
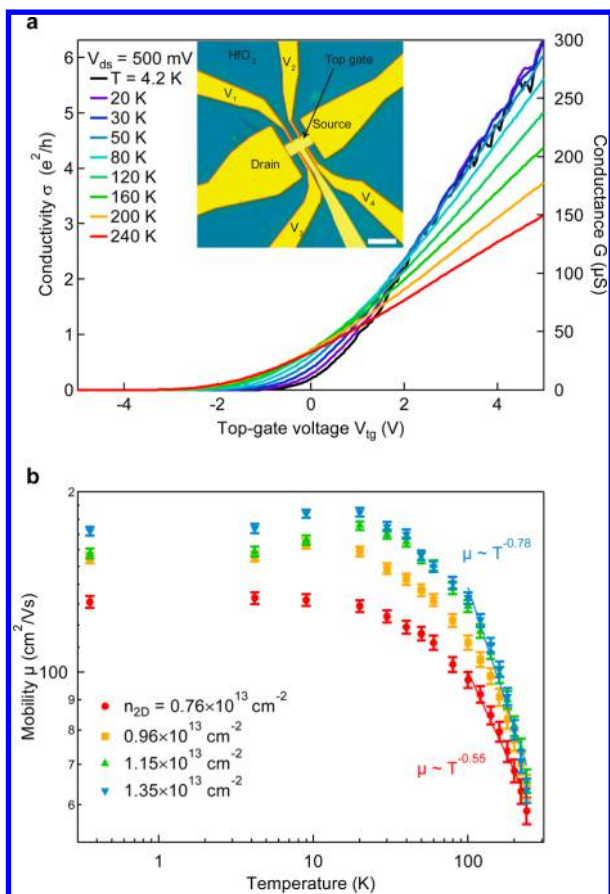
**Figure 2.** Mobility in single-layer MoS$_2$ encapsulated in HfO$_2$. (a) Conductivity $\sigma$ and conductance $G$ of MoS$_2$ as a function of top-gate voltage. For low values of $V_{tg}$, the conductivity decreases with temperature. Above $V_{tg} \approx 1-2$ V, single-layer MoS$_2$ enters a metallic state, with increasing conductivity as the temperature decreases. Inset: Optical image of the device[9] (scale bar 5 $\mu$m). (b) Field-effect mobility $\mu$ as a function of temperature. Above ~100 K, $\mu$ decreases due to phonon scattering. Adapted from ref 9. Copyright 2013 Nature Publishing Group.

high mobility and ambipolar behavior. The room-temperature on/off ratio was however rather low (~10) because of bulk conduction. This was soon followed by first devices based on single-layer MoS$_2$, which showed lower mobility (~3 cm$^2$/(V s)) than the bulk material and less than optimal switching characteristics for single layers.[7]

## ■ MoS$_2$ TRANSISTORS

The first implementation of a switchable single-layer MoS$_2$ transistor was demonstrated by Radisavljevic et al.[8] (Figure 1). In this device, 6.5 Å thick (Figure 1b) MoS$_2$ serves as the semiconducting channel. It is deposited on SiO$_2$ and covered by a 30 nm thick layer of HfO$_2$, which serves as the top-gate dielectric (Figure 1c). The transfer curves of the device are shown in Figure 1d. The transistor exhibits a current on/off ratio exceeding 10$^8$ at room temperature (Figure 1d). Besides this very high on/off ratio, the device exhibits off-state currents smaller than 100 fA (25 fA/$\mu$m). The high degree of electrostatic control is also reflected by the subthreshold slope $S = (\mathrm{d}(\log I_{ds})/\mathrm{d}V_{tg})^{-1}$, which is as low as 74 mV/dec. The pioneering work of Radisavljevic et al. showed that devices based on 2D semiconductors could reach competitive performance levels and was an important step toward the realization of
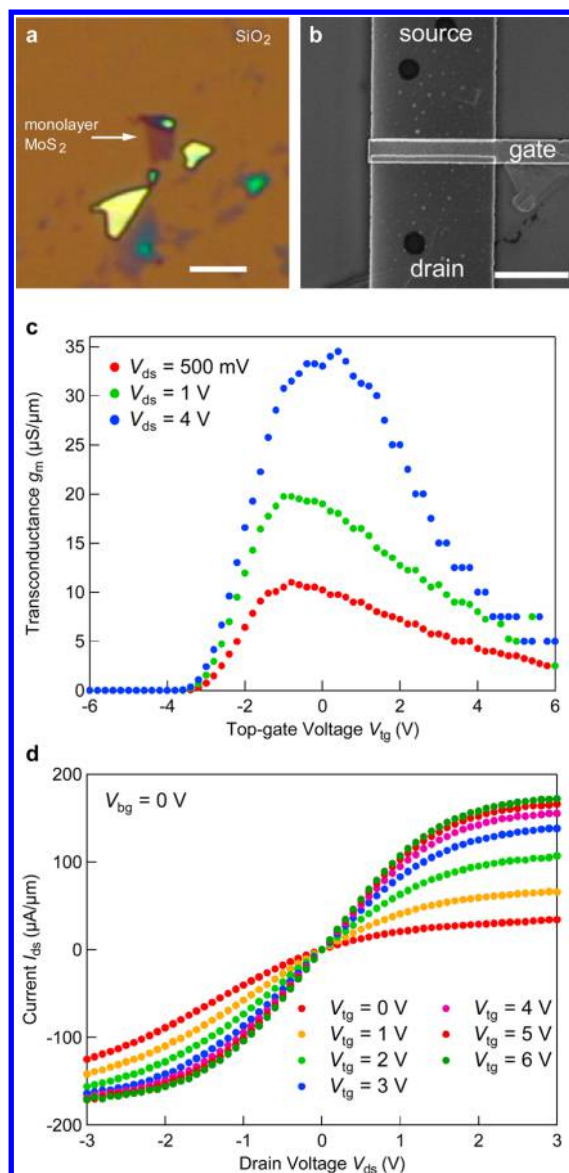


**Figure 3.** High-performance single-layer MoS$_2$ transistor. (a) Optical image of single-layer MoS$_2$ on SiO$_2$ (scale bar 5 $\mu$m). (b) SEM image of the device[12] (scale bar 2 $\mu$m). (c) Transconductance, $g_m = \mathrm{d}I_{ds}/\mathrm{d}V_{tg}$. (d) $I_{ds}-V_{ds}$ characteristics. For $V_{ds} > 2$ V, the drain current shows saturation with the drain–source conductivity, $g_{ds} = \mathrm{d}I_{ds}/\mathrm{d}V_{ds}$ close to zero ($g_{ds} < 2$ $\mu$S/$\mu$m). Reproduced from ref 12. Copyright 2012 American Chemical Society.

electronics and low stand-by power integrated circuits based on two-dimensional materials, with the additional potential for applications in flexible, transparent electronics.

In a subsequent study, Radisavljevic and Kis[9] studied the intrinsic mobility and conductivity of single-layer MoS$_2$ sandwiched in the dual-gated geometry (Figure 2). These material properties could not be deduced with the two-terminal geometry of the initial study[8] and require careful investigation with four-terminal and Hall-effect measurements (inset, Figure 2a). Figure 2a depicts the observed four-terminal conductivity $\sigma$ as a function of top-gate potential. At charge carrier densities $n_{2D}$ below ~1 × 10$^{13}$ cm$^{-2}$, the MoS$_2$ single-layer exhibits decreasing conductance as the temperature is decreased. For $n_{2D}$ larger than ~1 × 10$^{13}$ cm$^{-2}$, the conductance increases with decreasing temperature. This is the hallmark of a metal−insulator

transition (MIT).[9] Figure 2b depicts the temperature dependence of the extracted field-effect mobility for a single layer of $MoS_2$. In the range of 100 and 300 K, the mobility is phonon-limited and can be fitted to the power law $\mu \propto T^{-\gamma}$, with $\gamma$ in the range of 0.55−0.78. This result is much smaller than the theoretical prediction for a single-layer ($\gamma \approx 1.52$, ref 10) or bulk crystals ($\gamma \approx 2.6$, ref 5). The latter indicates that in addition to the quenching of the homopolar phonon mode, other mechanisms might influence the mobility of single-layer $MoS_2$ encapsulated in the dual-gated geometry.[11]

In a later study, Lembke and Kis[12] demonstrated high-performance single-layer $MoS_2$ transistors (Figure 3) with improved performance due to full-channel gating (Figure 3b). The resulting transconductance is shown in Figure 3c with the maximum of 34 $\mu S/\mu m$, while the output curves are shown in Figure 3d. Above $V_{ds} = 1$ V, the current carrying capacity of the $MoS_2$ charge-carrying channel is saturating, making this the first observation of drain current saturation in single-layer $MoS_2$ FETs, with the drain−source conductance close to zero ($g_{ds} < 2$ $\mu S/\mu m$). These results show that $MoS_2$ could be interesting not only for applications in digital electronics[13] but also for analogue applications where it could offer gain >10. Lembke and Kis also studied the breakdown current density in $MoS_2$, which is close to $5 \times 10^7$ $A/cm^2$. Considering that $MoS_2$ is a semiconductor, its extracted maximum current density is extremely high and 50 times larger than the limit set for metals by electromigration. This is due to strong intralayer Mo−S covalent bonds,[14,15] which are much stronger than metallic bonds. The study of Lembke and Kis demonstrates that single-layer $MoS_2$ could be used in analogue circuit applications where it could provide power gain and support large current densities. High-frequency operation of $MoS_2$ FETs was also recently demonstrated by Krasnozhon et al. (Figure 4), who demonstrated current, voltage, and power gains in the gigahertz range in transistors based on 1−3 layer thick $MoS_2$ with a channel length of 240 nm.[16] This shows that the mobility of $MoS_2$ is large enough to allow device operation in the technologically relevant gigahertz frequency range. These performance figures are currently limited rather by the contact resistance and relatively large gate lengths, and scaling is expected to result in further improvements of the operating speed.

## ■ $MoS_2$ LOGIC CIRCUITS AND AMPLIFIERS

After the demonstration of FETs based on single-layer $MoS_2$, Radisavljevic et al.[13,17] realized electronic circuits based on the dual-gate geometry, including the first $MoS_2$ inverter demonstrated in 2011. Figure 5a shows an example of a circuit consisting of six FETs connected in series and fabricated on the same piece of single-layer $MoS_2$. A similar device was successfully operated as an inverter, the fundamental building block of digital electronics consisting of two FETs connected in series (Figure 5b) with the common electrode serving as the output and the gate of a transistor as the input (Inset Figure 5c). The circuit is characterized by a voltage gain larger than 4 (Figure 5c). This indicates that inverters based on single-layer $MoS_2$ FETs can be used for the fabrication of more complex circuits, consisting of cascaded inverters, where a gain larger than unity is required. Finally, single-layer $MoS_2$ transistors were also employed for the realization of analog circuits,[17] such as a small signal amplifier, with gain up to 6.9 (Figure 5d).
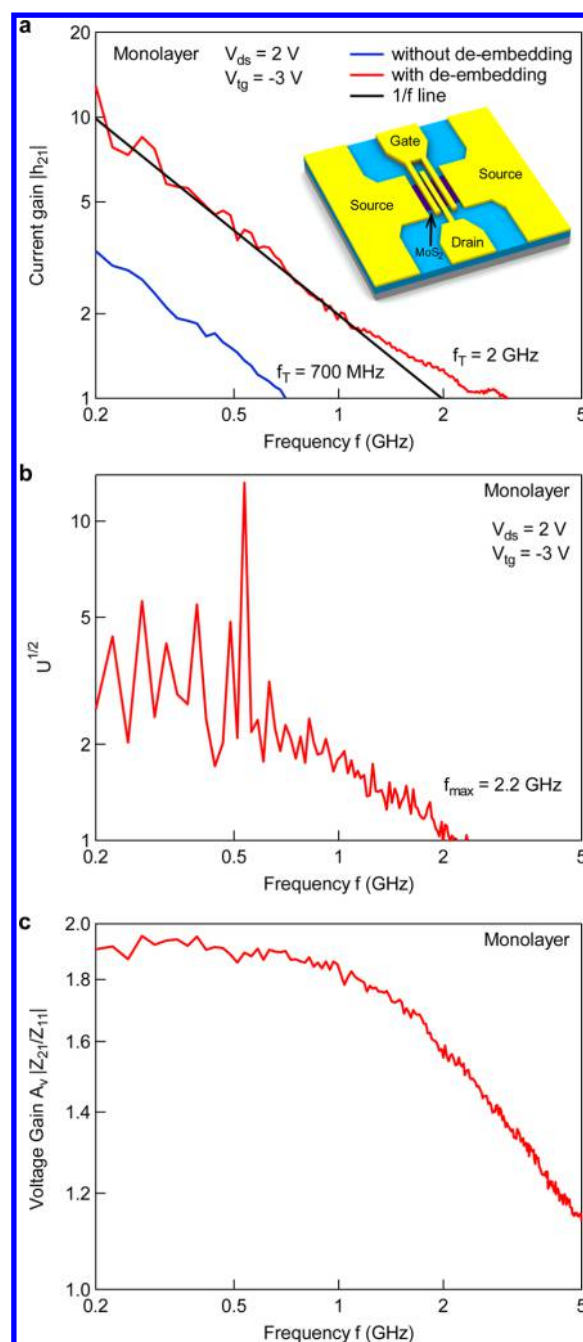


**Figure 4.** RF performance of $MoS_2$ transistors. (a) Small-signal current gain $h_{21}$ as a function of frequency for devices based on single-layer $MoS_2$ with the cutoff frequency $f_T = 2$ GHz. (b) Mason's unilateral gain $U$ as a function of frequency. Maximum frequency of oscillation $f_{max} = 2.2$ GHz is extracted. (c) Voltage gain $|Z_{21}/Z_{11}|$ as a function of frequency showing gain higher than 1 up to 5 GHz. Adapted with permission from ref 16. Copyright 2014 American Chemical Society.

## ■ FLASH MEMORY

Combining the high conductivity of graphene with the semiconducting properties of single-layer $MoS_2$ represents a unique opportunity for creating high-performing devices with advanced functionalities, such as all-2D memory devices. Bertolazzi et al.[18] demonstrated a nonvolatile memory cell based on $MoS_2$/graphene heterostructures. The device architecture, which resembles that of a floating gate FET, its electrical connections, and its
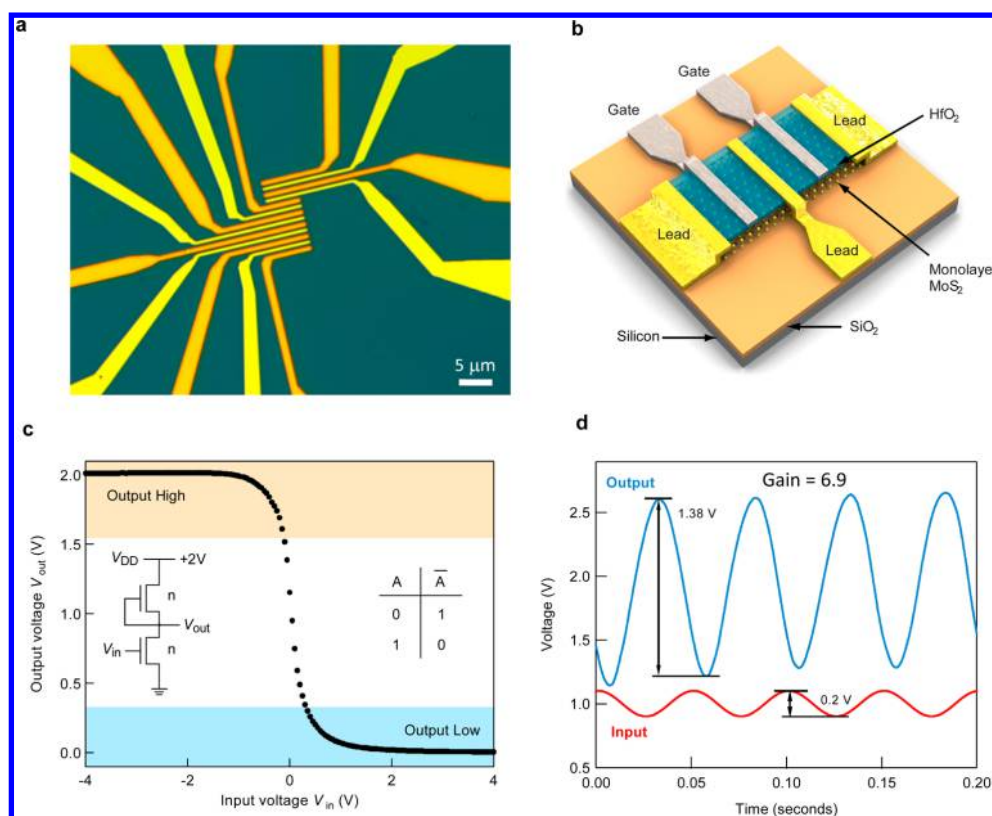
**Figure 5.** Electronic circuits based on single-layer $MoS_2$. (a) Electronic circuit containing six field-effect transistors integrated on the same single-layer $MoS_2$ flake. Adapted with permission from ref 3. Copyright 2012 Nature Publishing Group. (b) Three dimensional schematics of a device consisting of two top-gated transistors. (c) Output voltage versus input voltage characteristic of the device represented in panel b, which functions as a digital inverter. The insets show the circuit diagram (left) and the corresponding logic inversion operation (right). Adapted with permission from ref 13. Copyright 2011 American Chemical Society. (d) An equivalent $MoS_2$-based electronic circuit was employed in ref 17 to demonstrate analog small-signal amplifiers with voltage gain $G$ larger than 4. Adapted with permission from ref 17. Copyright 2012 AIP Publishing LLC.

fabrication procedure are reported in Figure 6a−c. Single-layer $MoS_2$ acts as the transistor channel, and graphene electrodes are used to inject and collect the charge carriers. A piece of multilayer graphene, ∼4 nm thick, is employed as the charge trapping layer (floating gate) and is separated from the semiconducting channel by a 6 nm thick $HfO_2$ layer, serving as the tunnel oxide. The device is completed with the deposition of the control oxide and the control gate electrode.

For the first time, it was also shown that graphene can be used as a contact material to single-layer $MoS_2$, resulting in ohmic-like $I_{ds}$ vs $V_{ds}$ output characteristics at room-temperature (Figure 6d). This result suggests the possibility to exploit the tunability of the graphene work function, e.g. by means of chemical functionalization or electrostatic doping, to develop efficient contacts and highly conducting graphene interconnects in advanced electronic circuits.

Due to the atomic scale thickness of single-layer $MoS_2$ and its large bandgap, the transistor operation was found to be very sensitive to the presence of charges in the floating gate. The proof-of-concept device by Bertolazzi et al. showed a program/erase current ratio as high as $10^4$ (Figure 6e), which is considerably higher than what has been reported for memory devices employing graphene as the active material. The observed large memory window (>8 V) revealed the possibility for engineering 2D memory cells with multilevel data storage capability.

## OPTOELECTRONIC DEVICES

The direct bandgap[19,20] of single-layer $MoS_2$ makes it suitable for optoelectronic applications. First single-layer $MoS_2$ photo-transistors exhibited a photoresponsivity of 7.5 mA/W.[21] Multilayer $MoS_2$ devices[22,23] show higher photoresponsivity of ∼100 mA/W, comparable to Si-based photodetectors. However, relatively low mobility (0.1 $cm^2$/(V s)) and high contact resistance in these devices offset the inherent advantage of using a material with direct bandgap. Lopez-Sanchez et al.[24] demonstrated an ultrasensitive single-layer $MoS_2$ photodetector due to improved mobility and contact quality (Figure 7). The output curves depicted in Figure 7b show an increase of drain current by several orders of magnitude as the device is illuminated, proving photoresponse. As shown in Figure 7c, in the dark the device shows behavior typical of n-type $MoS_2$ FETs. When the device is illuminated, the device current increases for both the on and off states. This indicates that photocurrent dominates over thermionic and tunneling currents. Figure 7d shows the device photoresponsivity, reaching 880 A/W. Furthermore, the presence of a bandgap and high degree of electrostatic control allows the photo-transistor to be efficiently turned off, resulting in a noise level lower than in commercial state-of-the-art Si avalanche photodiodes.

Sundaram et al.[25] demonstrated that single-layer $MoS_2$ can be used as light emitter. While their study served as a proof-of-principle, the device was limited by a relatively high power
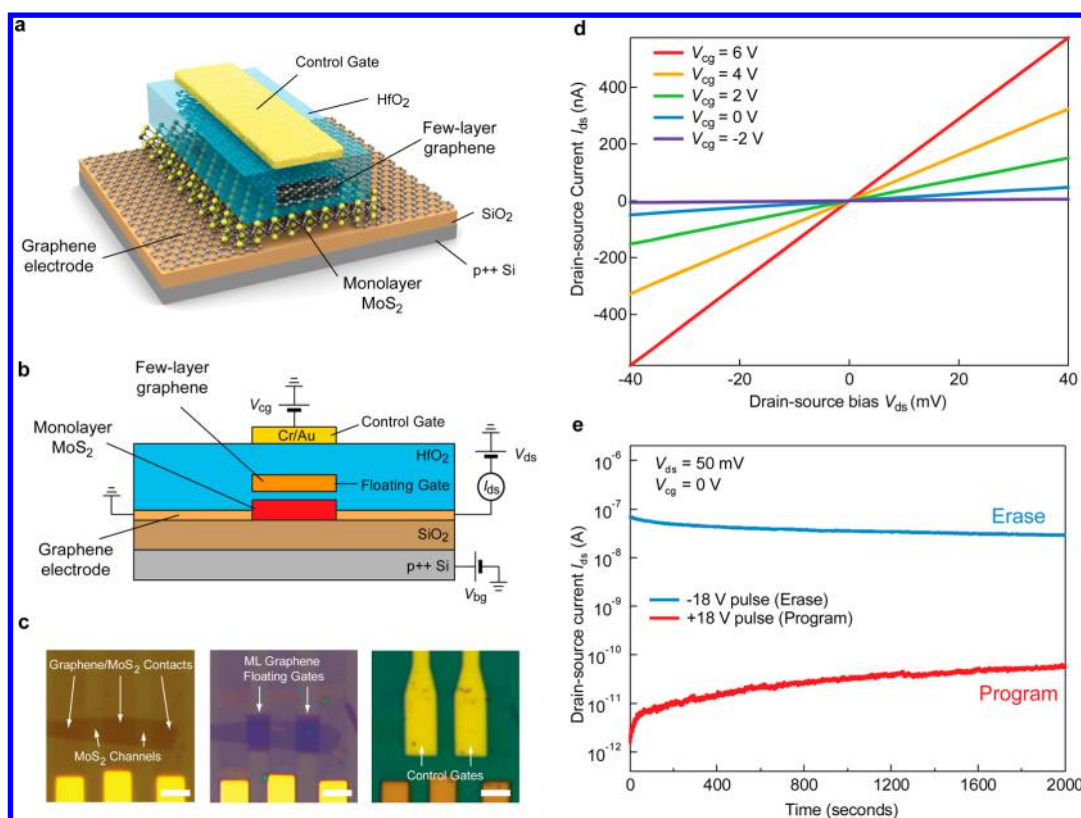
**Figure 6.** Flash memory device based on MoS$_2$/graphene heterostructures. (a) Three dimensional representation of the MoS$_2$/graphene floating gate transistor. (b) Schematic of the device comprising a single-layer MoS$_2$ semiconducting channel, graphene contacts, and multilayer graphene floating gate. (c) Optical micrographs of two floating gate transistors at different stages of the fabrication process. (d) Output curves of the floating gate transistor showing room-temperature ohmic-like behavior for graphene contacts to single-layer MoS$_2$. (e) Time-dependent behavior of the drain−source current for Program and Erase states. The magnitude of the Erase current at low bias ($V_{ds}$ = 50 mV) is more than 3 orders of magnitude higher than the Program current, due to the high electrostatic sensitivity of the 2D channel to the charges trapped in the floating gate. Reproduced from ref 18. Copyright 2013 American Chemical Society.

threshold for light emission and only a small portion of the device, restricted to the contact edge, was active in electroluminescence.[25] A way to overcome these limiting factors is to build light-emitting diodes based on vertical pn-junctions, resulting in an increase of the junction's area. Lopez-Sanchez et al.[26] demonstrated a new geometry in the form of a vertical heterostructure composed of n-type MoS$_2$ serving as electron injection layer and p-type Si serving as the hole injection layer (Figure 8). Figure 8a shows the current versus bias characteristic of the MoS$_2$/Si heterojunction diode (Inset Figure 8a), exhibiting rectifying behavior. This shows that classical diodes and related optoelectronic devices could be fabricated using a combination of atomically thin 2D and classical 3D semiconductors. The electroluminescent emission intensity map is shown in Figure 8b. Most of the heterojunction surface is active in light emission. This is attractive from the practical point of view because the total emitted light intensity can be scaled up easily by increasing the device area. Figure 8c shows the observed electroluminescence spectrum, closely matched to the MoS$_2$ PL spectrum. This shows that the relevant energy for the radiative recombination process in the MoS$_2$/Si heterojunction is the direct bandgap in single-layer MoS$_2$. The heterojunction diode can also convert incident light into electrical current with an external quantum efficiency of 4.4% and a broad spectral response.[26]

## ■ MECHANICAL PROPERTIES

Measurements of mechanical properties of MoS$_2$ showed that these materials also have a strong potential in high-end flexible and transparent electronics. Bertolazzi et al.[15] reported the first measurements of the in-plane stiffness and breaking strength of single and bilayer sheets of MoS$_2$ by means of nanoindentation experiments performed with the tip of an atomic-force microscope (AFM) on free-standing MoS$_2$ membranes (Figure 9). Such measurements provide simultaneous access to different material properties, such as the 2D Young's modulus ($E^{2D}$), the pre-tension ($\sigma_0^{2D}$) of the membrane, and its breaking strength ($\sigma_{MAX}^{2D}$), which in the case of defect-free material is directly related to the intrinsic strength of the interatomic bonds.

Free-standing MoS$_2$ membranes were fabricated on SiO$_2$/Si substrates by transferring atomically thin sheets of MoS$_2$ over an array of microfabricated circular holes, as shown in Figure 9a,b. During the indentation experiment, the AFM tip was pushed against the center of the membrane, and the cantilever deflection $\Delta z_c$ was monitored, resulting in force $F$ versus membrane-deflection $\delta$ curves such as those shown in Figure 9c. A semiempirical model was used to describe the curves, which assumes that the suspended MoS$_2$ sheets behave as a clamped circular membrane, made of a linear isotropic elastic material. Fitting the experimental curves with this model allows the extraction of the 2D membrane pre-tension $\sigma_0^{2D}$ (in the 0.02−0.2 N/m range) and of the Young's modulus $E = ((E^{2D})/t)$ of

F

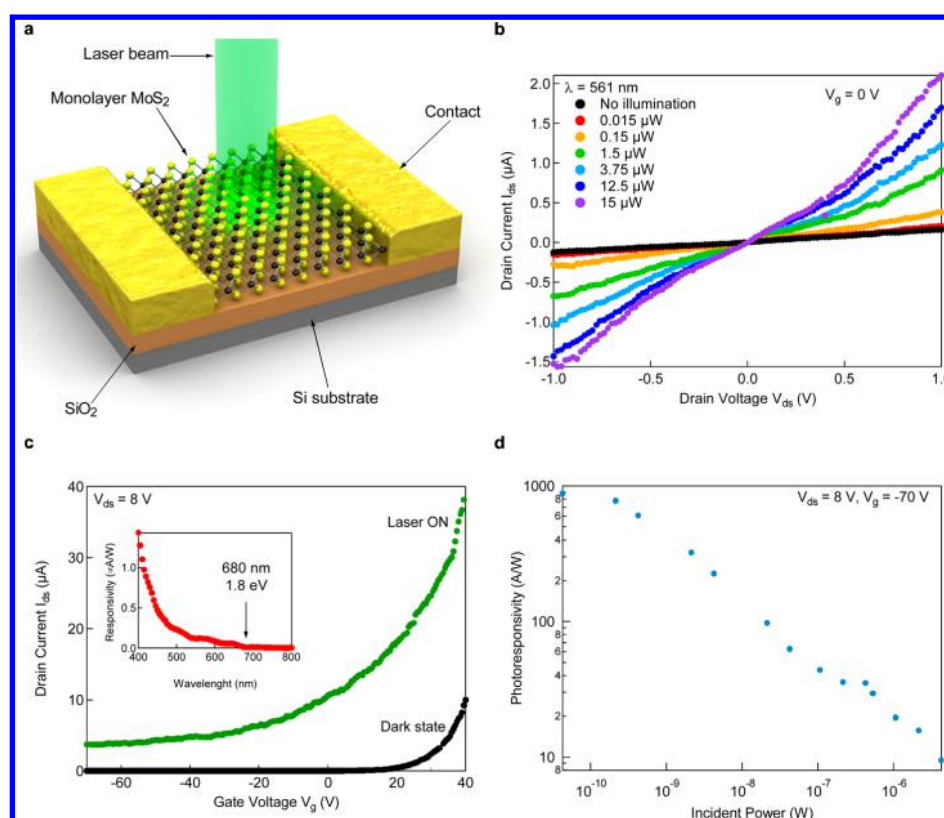dx.doi.org/10.1021/ar500274q | Acc. Chem. Res. XXXX, XXX, XXX−XXX

**Figure 7.** Ultrasensitive single-layer MoS$_2$ photodetector. (a) Three-dimensional schematic view of the device studied by Lopez-Sanchez et al.[24] (b) Output curves in the dark and under illumination. Increasing illumination power results in enhanced current due to electron−hole pair generation by light absorption in the direct bandgap of single-layer MoS$_2$. (c) Transfer curves in the dark and illuminated state. Inset: Photoresponsivity as a function of illumination wavelength. (d) Photoresponsivity of the MoS$_2$ phototransistor showing ultrahigh sensitivity. The device exhibits a photoresponsivity of 880 A/W for an illumination power of 150 pW ($\sim$24 $\mu$W/cm$^2$). Adapted with permission from ref 24. Copyright 2013 Nature Publishing Group.

the ultrathin MoS$_2$ sheets. The membranes were further deformed up to the breaking point and the forces at which the rupture occurred were recorded (black and blue crosses in Figure 9c). After the occurrence of the breaking event, a hole was produced in the center of the membrane, at the location where the AFM tip punctured the MoS$_2$ sheet. Figure 9d,e shows intermittent-contact AFM topography images of the same free-standing MoS$_2$ membrane before and after performing the stretching and breaking experiments.

It was found that the Young's modulus of single-layer MoS$_2$ is $\sim$270 GPa, higher than that of steel ($\sim$205 GPa). The Young's modulus of singe-layer MoS$_2$ was found to be higher than that of bulk MoS$_2$ ($\sim$240 GPa), most likely due to defects, interlayer sliding, or the absence of stacking faults in single-layers. Castellanos-Gomez et al.[27] performed similar experiments on multilayer MoS$_2$ with thickness ranging from 5 to 25 layers and obtained a Young's modulus of 330 $\pm$ 70 GPa. Recent quantum-chemical molecular dynamics simulations performed by Lorenz et al.[28] show excellent agreement with the experimental observations of Bertolazzi et al. First-principles calculations by Li[29] also predicted that ultrathin sheets of MoS$_2$ are characterized by a biaxial elastic modulus of $\sim$250 GPa.

The breaking strength of single- and bilayer MoS$_2$ was between 6% and 11% of their Young's modulus, which represents the upper theoretical limit of a material's breaking strength and reflects the intrinsic properties of its interatomic bonds.[15] This suggests that MoS$_2$ can be suitable for integration with flexible

plastic substrates, such as polyimide, whose maximum strain before failure is $\sim$7%.

All these results indicate that single-layer MoS$_2$ is at present the strongest and thinnest semiconducting material ever measured. Its ultimate thickness, low mass, and semiconducting energy gap could be exploited for building nano-electromechanical systems (NEMS) with new functionalities. One first example was given by Castellanos-Gomez et al.,[30] who demonstrated mechanical resonators based on single-layer MoS$_2$ membranes operating in the tension-dominated regime with resonance frequencies up to 30 MHz and a quality factor $\sim$55.

Further research is needed in order to explore the mechanical properties of other TMDs characterized by different electronic/optical properties that may be complementary to those of MoS$_2$.

Single-layer MoS$_2$, combined with conducting graphene and insulating BN, could be employed as semiconducting channel in all-2D FETs integrated on flexible substrates. Lee et al.[31] recently demonstrated MoS$_2$ FETs on flexible polymer substrates, which incorporate heterostructures of graphene and BN and show unaffected electronic mobility at strain levels of up to 1.5%. These results are a consequence of the excellent mechanical properties of 2D materials, which stem from their strong in-plane interatomic bonds.
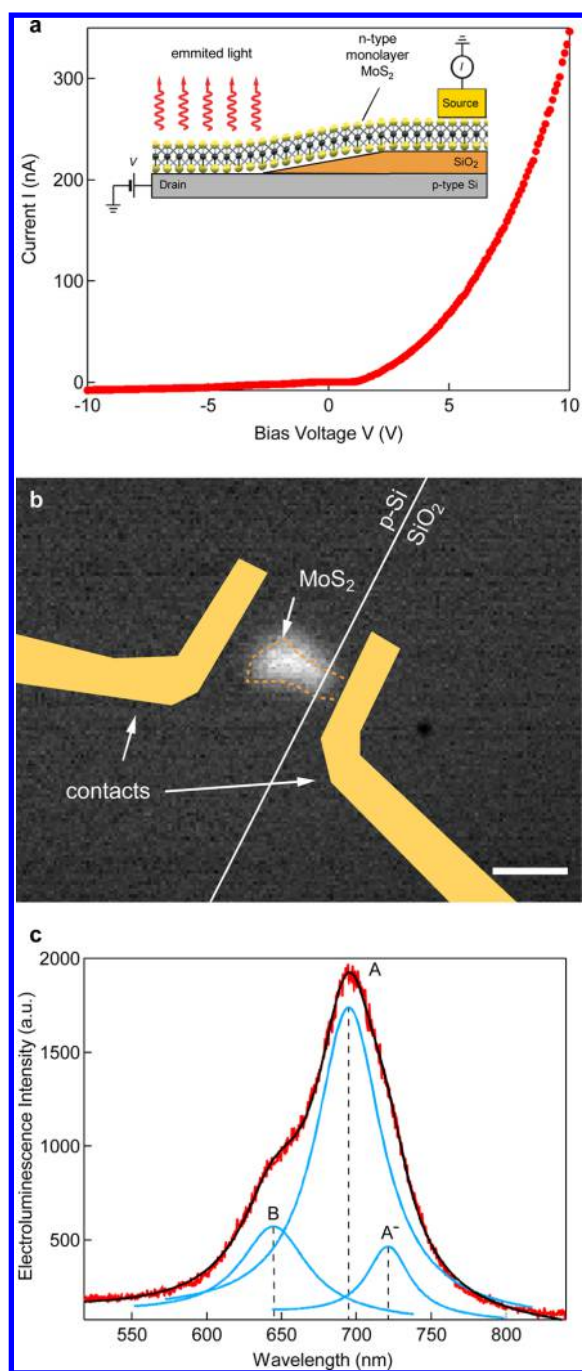
**Figure 8.** pn-Junction incorporating single-layer MoS$_2$. (a) Current vs bias curve of MoS$_2$/Si heterojunction diode studied by Lopez-Sanchez et al.[26] Inset: Cross-sectional view of the device. Electrons are injected from n-type MoS$_2$, while holes are injected from the p-Si substrate. (b) Intensity map showing electroluminescent emission with super-imposed outline of the device components. The entire surface of the heterojunction emits light (scale bar 5 $\mu$m). (c) Electroluminescence spectrum acquired under a forward bias $V$ = 15 V ($I$ = 1.8 $\mu$A). The spectrum is fitted with three Lorentzian lines that correspond to the A and B excitons of MoS$_2$ and the A$^-$ trion resonance. Reproduced from ref 26. Copyright 2014 American Chemical Society.

### ■ THERMAL PROPERTIES

The thermal and thermoelectric properties[32−34] of single-layer MoS$_2$ have been investigated to assess its potential for applications in thermal nanodevices, such as on-chip power generators and nanosystems for waste thermal energy harvesting. Using temperature-dependent Raman spectroscopy on sus-pended sheets, Yan et al.[32] extracted the thermal conductivity of single-layer MoS$_2$ (∼34.5 W/mK), which was found to be significantly lower than that of graphene. Buscema et al.[33] mea-sured the Seebeck coefficient in back-gated MoS$_2$ transistors and obtained a large tunable value, which could be varied between $-4 \times 10^2$ $\mu$V/K and $-1 \times 10^5$ $\mu$V/K by a gate voltage. This result shows that single-layer MoS$_2$ can be suitable for the aforementioned thermoelectric applications. Recent theoretical calculations by Huang et al.[34] also confirm that 2D TMDs are promising thermoelectric materials.

### ■ PROSPECTS AND CHALLENGES

In the coming years, several issues need to be addressed for MoS$_2$ devices to become mature. There is at this point no control over intrinsic doping levels in MoS$_2$. Possible doping strategies include the introduction of atoms (F, Cl, Re, etc.) substituting atoms of the crystal's lattice (Mo, S) during the growth process as well as doping by adsorption of donor or acceptor molecules.[35] Controlled doping will open up the route to achieve p-type or ambipolar behavior in single-layer MoS$_2$. Understanding how to make good electrical contacts to MoS$_2$ is also lagging. One strategy to reduce the contact resistance in 2D MoS$_2$/metal junctions could be based on heavily doping of the contact region by donor molecules.[36] Another possibility is based on phase engineering of the MoS$_2$ region below the contact, for example, by converting the semiconductor into metallic 1T phase by treatment with *n*-butyl lithium.[37] Another problem that needs to be addressed is related to atomic-layer deposition (ALD) of high-$\kappa$ dielectrics in extremely scaled devices. Since the presence of hydroxyl groups is crucial for the quality of the ALD deposition and pristine MoS$_2$ lacks out-of-plane covalent functional groups, surface functionalization might be required to fabricate extremely scaled devices.[38] On the basis of theoretical predictions[39] there is still much oppor-tunity for improving the charge carrier mobility. Therefore, reducing charge impurity scattering centers at the dielectric/MoS$_2$ interfaces as well as within the material itself might result in devices of significantly enhanced performance.

### ■ CONCLUSION

The discussed results indicate that MoS$_2$ is indeed a very promising material for practical electronic and optoelectronic applications. Figure 10 depicts a schematic comparison of the current on/off ratio, the bandgap, and the field-effect mobility of several materials suitable for electronic and optoelectronic applications, including traditional semiconductors and novel flexible materials. Each material class has its strength and weak-nesses and which material to select for a given application depends on its specification. The particular advantages of single-layer MoS$_2$ include chemical stability, planar geometry, high bandgap, very high on/off ratio, competitive mobility, flexibility, and transparency. In combination with other 2D materials such as graphene and insulating layered materials (e.g., BN), MoS$_2$ adds to a repertoire suitable to construct elec-tronic and optoelectronic heterostructures.[40] Together with recent developments in large-scale production techniques,[41] MoS$_2$ could potentially be incorporated in roll-to-roll processes to fabricate inexpensive, flexible, and transparent 2D devices.
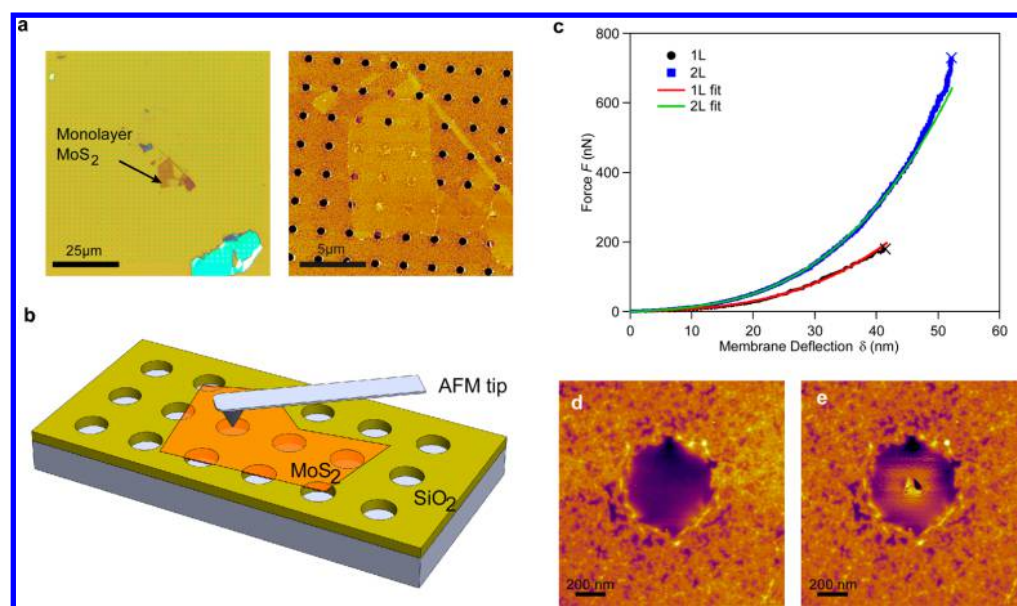
**Figure 9.** Nanoindentation of suspended MoS$_2$ sheets. (a) Optical micrograph (left) of single-layer MoS$_2$ deposited on a SiO$_2$/Si substrate with holes. AFM image (right) showing the MoS$_2$ flake forming a series of free-standing membranes. (b) Schematics of the AFM nanoindentation experiment. (c) Force $F$ versus membrane-deflection, $\delta$, curves for single- and bilayer MoS$_2$. The breaking events occur at the points marked with the black (single-layer) and blue (bilayer) crosses. (d) AFM image of suspended single-layer MoS$_2$ before the indentation process and (e) after the occurrence of the breaking event. Adapted with permission from ref 15. Copyright 2011 American Chemical Society.
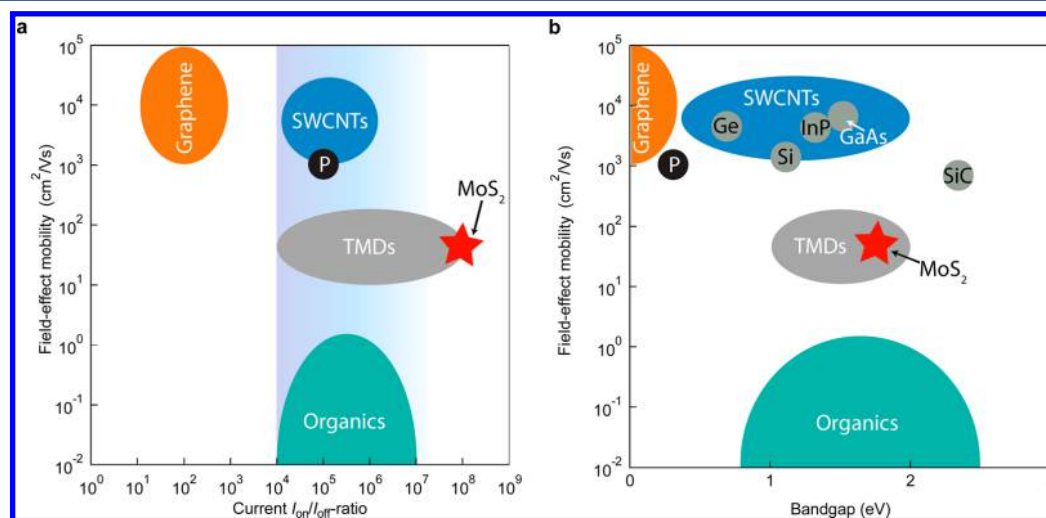


**Figure 10.** Schematic comparison of single-layer MoS$_2$ with other materials suitable for electronic and optoelectronic applications. Field-effect mobility as a function of (a) current on/off ratio and (b) electronic bandgap. For practical applications, an on/off ratio on the order of $10^4-10^7$ is desirable.[43] We compare the properties of graphene (including its bilayer),[44] multilayered (10 nm thick) black phosphorus (P),[45] single walled carbon nanotubes (SWNTs),[46] few-layered transition metal dichalcogenides (TMDs),[3] organic semiconductors,[47] and several traditional semiconductors[48] with single-layer MoS$_2$ (red star).

■ **AUTHOR INFORMATION**

**Corresponding Author**

*Andras Kis. E-mail: andras.kis@epfl.ch.

**Notes**

The authors declare no competing financial interest.

**Biographies**

**Dominik Lembke** was born in 1984 in Munich, Germany. He graduated from Ludwig Maximilian University Munich with a Diplom in Physics (2010) and holds a Technology Management degree from Technical University Munich (2008). He is currently pursuing research towards his Ph.D. in Physics in the laboratory of Prof. Andras Kis at EPFL. His work focuses on electrical properties and applications of two-dimensional MoS$_2$ transistors. His general research interests include novel materials suitable for flexible, transparent electronics.

**Simone Bertolazzi** was born in 1985 in Verona, Italy. He received the Laurea degree in 2007 from Politecnico di Milano (Engineering Physics) and M.Sc. degree in 2010 from both Politecnico di Milano and École

I

dx.doi.org/10.1021/ar500274q | *Acc. Chem. Res.* XXXX, XXX, XXX−XXX

Polytechnique de Montréal (Engineering Physics). He is presently a Ph.D. student in the laboratory of Prof. Andras Kis at EPFL. The focus of his doctoral work is on the mechanical and electronic properties of two-dimensional materials for application in flexible electronics.

**Andras Kis** was born in 1975 in Zagreb, Croatia. He graduated in Physics from the University of Zagreb in 1999 and obtained a Ph.D. in Physics from EPFL (École Polytechnique Fédérale de Lausanne) in 2003 after which he worked as a postdoctoral researcher at the University of California, Berkeley, in the group of Prof. Zettl. He has joined EPFL as faculty in 2008 where he formed a new research group with the aim of studying 2D materials beyond graphene, with a strong emphasis on transition metal dichalcogenide based electronics.

## ■ REFERENCES

(1) Schwierz, F. Graphene transistors. *Nat. Nanotechnol.* **2010**, *5*, 487−496.

(2) Colinge, J.-P. Multiple-gate SOI MOSFETs. *Solid-State Electron.* **2004**, *48*, 897−905.

(3) Wang, Q. H.; Kalantar-Zadeh, K.; Kis, A.; Coleman, J. N.; Strano, M. S. Electronics and optoelectronics of two-dimensional transition metal dichalcogenides. *Nat. Nanotechnol.* **2012**, *7*, 699−712.

(4) Frindt, R. F.; Yoffe, A. D. Physical properties of layer structures: Optical properties and photoconductivity of thin crystals of molybdenum disulphide. *Proc. R. Soc. London, Ser. A* **1963**, *273*, 69−83.

(5) Fivaz, R.; Mooser, E. Mobility of charge carriers in semi-conducting layer structures. *Phys. Rev.* **1967**, *163*, 743−755.

(6) Podzorov, V.; Gershenson, M. E.; Kloc, C.; Zeis, R.; Bucher, E. High-mobility field-effect transistors based on transition metal dichalcogenides. *Appl. Phys. Lett.* **2004**, *84*, 3301−3303.

(7) Novoselov, K. S.; Jiang, D.; Schedin, F.; Booth, T. J.; Khotkevich, V. V.; Morozov, S. V.; Geim, A. K. Two-dimensional atomic crystals. *Proc. Natl. Acad. Sci. U.S.A.* **2005**, *102*, 10451−10453.

(8) Radisavljevic, B.; Radenovic, A.; Brivio, J.; Giacometti, V.; Kis, A. Single-layer $MoS_2$ transistors. *Nat. Nanotechnol.* **2011**, *6*, 147−197.

(9) Radisavljevic, B.; Kis, A. Mobility engineering and a metal-insulator transition in monolayer $MoS_2$. *Nat. Mater.* **2013**, *12*, 815−820.

(10) Kaasbjerg, K.; Thygesen, K. S.; Jacobsen, K. W. Phonon-limited mobility in n-type single-layer $MoS_2$ from first principles. *Phys. Rev. B* **2012**, *85*, 115317.

(11) Ong, Z.-Y.; Fischetti, M. V. Mobility enhancement and temperature dependence in top-gated single-layer $MoS_2$. *Phys. Rev. B* **2013**, *88*, 165316.

(12) Lembke, D.; Kis, A. Breakdown of high-performance monolayer $MoS_2$ transistors. *ACS Nano* **2012**, *6*, 10070−10075.

(13) Radisavljevic, B.; Whitwick, M. B.; Kis, A. Integrated circuits and logic operations based on single-layer $MoS_2$. *ACS Nano* **2011**, *5*, 9934−9938.

(14) Ataca, C.; Şahin, H.; Ciraci, S. Stable, single-layer MX2 transition-metal oxides and dichalcogenides in a honeycomb-like structure. *J. Phys. Chem. C* **2012**, *116*, 8983−8999.

(15) Bertolazzi, S.; Brivio, J.; Kis, A. Stretching and breaking of ultrathin $MoS_2$. *ACS Nano* **2011**, *5*, 9703−9709.

(16) Krasnozhon, D.; Lembke, D.; Nyffeler, C.; Leblebici, Y.; Kis, A. $MoS_2$ transistors operating at gigahertz frequencies. *Nano Lett.* **2014**, *14*, 5905−5911.

(17) Radisavljevic, B.; Whitwick, M. B.; Kis, A. Small-signal amplifier based on single-layer $MoS_2$. *Appl. Phys. Lett.* **2012**, *101*, No. 043103.

(18) Bertolazzi, S.; Krasnozhon, D.; Kis, A. Nonvolatile memory cells based on $MoS_2$/graphene heterostructures. *ACS Nano* **2013**, *7*, 3246−3252.

(19) Splendiani, A.; Sun, L.; Zhang, Y.; Li, T.; Kim, J.; Chim, C.-Y.; Galli, G.; Wang, F. Emerging photoluminescence in monolayer $MoS_2$. *Nano Lett.* **2010**, *10*, 1271−1275.

(20) Mak, K. F.; Lee, C.; Hone, J.; Shan, J.; Heinz, T. F. Atomically thin $MoS_2$: A new direct-gap semiconductor. *Phys. Rev. Lett.* **2010**, *105*, No. 136805.

(21) Yin, Z.; Li, H.; Li, H.; Jiang, L.; Shi, Y.; Sun, Y.; Lu, G.; Zhang, Q.; Chen, X.; Zhang, H. Single-layer $MoS_2$ phototransistors. *ACS Nano* **2011**, *6*, 74−80.

(22) Lee, H. S.; Min, S.-W.; Chang, Y.-G.; Park, M. K.; Nam, T.; Kim, H.; Kim, J. H.; Ryu, S.; Im, S. $MoS_2$ nanosheet phototransistors with thickness-modulated optical energy gap. *Nano Lett.* **2012**, *12*, 3695−3700.

(23) Choi, W.; Cho, M. Y.; Konar, A.; Lee, J. H.; Cha, G.-B.; Hong, S. C.; Kim, S.; Kim, J.; Jena, D.; Joo, J.; Kim, S. High-detectivity multilayer $MoS_2$ phototransistors with spectral response from ultraviolet to infrared. *Adv. Mater.* **2012**, *24*, 5832−5836.

(24) Lopez-Sanchez, O.; Lembke, D.; Kayci, M.; Radenovic, A.; Kis, A. Ultrasensitive photodetectors based on monolayer $MoS_2$. *Nat. Nanotechnol.* **2013**, *8*, 497−501.

(25) Sundaram, R. S.; Engel, M.; Lombardo, A.; Krupke, R.; Ferrari, A. C.; Avouris, P.; Steiner, M. Electroluminescence in single layer $MoS_2$. *Nano Lett.* **2013**, *13*, 1416−1421.

(26) Lopez-Sanchez, O.; Llado, E. A.; Koman, V.; Morral, A. F. I.; Radenovic, A.; Kis, A. Light generation and harvesting in a van der Waals heterostructure. *ACS Nano* **2014**, *8*, 3042−3048.

(27) Castellanos-Gomez, A.; Poot, M.; Steele, G. A.; van der Zant, H. S. J.; Agraït, N.; Rubio-Bollinger, G. Elastic properties of freely suspended $MoS_2$ nanosheets. *Adv. Mater.* **2012**, *24*, 772−775.

(28) Lorenz, T.; Joswig, J.-O.; Seifert, G. Stretching and breaking of monolayer $MoS_2$—an atomistic simulation. *2D Mater.* **2014**, *1*, 011007.

(29) Li, T. Ideal strength and phonon instability in single-layer $MoS_2$. *Phys. Rev. B* **2012**, *85*, 235407.

(30) Castellanos-Gomez, A.; van Leeuwen, R.; Buscema, M.; van der Zant, H. S. J.; Steele, G. A.; Venstra, W. J. Single-layer $MoS_2$ mechanical resonators. *Adv. Mater.* **2013**, *25*, 6719−6723.

(31) Lee, G.-H.; Yu, Y.-J.; Cui, X.; Petrone, N.; Lee, C.-H.; Choi, M. S.; Lee, D.-Y.; Lee, C.; Yoo, W. J.; Watanabe, K.; Taniguchi, T.; Nuckolls, C.; Kim, P.; Hone, J. Flexible and transparent $MoS_2$ field-effect transistors on hexagonal boron nitride-graphene heterostructures. *ACS Nano* **2013**, *7*, 7931−7936.

(32) Yan, R.; Simpson, J. R.; Bertolazzi, S.; Brivio, J.; Watson, M.; Wu, X.; Kis, A.; Luo, T.; Hight Walker, A. R.; Xing, H. G. Thermal conductivity of monolayer molybdenum disulfide obtained from temperature-dependent Raman spectroscopy. *ACS Nano* **2014**, *8*, 986−993.

(33) Buscema, M.; Barkelid, M.; Zwiller, V.; van der Zant, H. S. J.; Steele, G. A.; Castellanos-Gomez, A. Large and tunable photothermo-electric effect in single-layer $MoS_2$. *Nano Lett.* **2013**, *13*, 358−363.

(34) Huang, W.; Luo, X.; Gan, C. K.; Quek, S. Y.; Liang, G. Theoretical study of thermoelectric properties of few-layer $MoS_2$ and $WSe_2$. *Phys. Chem. Chem. Phys.* **2014**, *16*, 10866−10874.

(35) Dolui, K.; Rungger, I.; Das Pemmaraju, C.; Sanvito, S. Possible doping strategies for $MoS_2$ monolayers: An ab initio study. *Phys. Rev. B* **2013**, *88*, 075420.

(36) Kiriya, D.; Tosun, M.; Zhao, P.; Kang, J. S.; Javey, A. Air-stable surface charge transfer doping of $MoS_2$ by benzyl viologen. *J. Am. Chem. Soc.* **2014**, *136*, 7853−7856.

(37) Kappera, R.; Voiry, D.; Yalcin, S. E.; Branch, B.; Gupta, G.; Mohite, A. D.; Chhowalla, M. Phase-engineered low-resistance contacts for ultrathin $MoS_2$ transistors. *Nat. Mater.* **2014**, *13*, 1128−1134.

(38) McDonnell, S.; Brennan, B.; Azcatl, A.; Lu, N.; Dong, H.; Buie, C.; Kim, J.; Hinkle, C. L.; Kim, M. J.; Wallace, R. M. $HfO_2$ on $MoS_2$ by atomic layer deposition: Adsorption mechanisms and thickness scalability. *ACS Nano* **2013**, *7*, 10354−10361.

(39) Kaasbjerg, K.; Thygesen, K. S.; Jauho, A.-P. Acoustic phonon limited mobility in two-dimensional semiconductors: Deformation potential and piezoelectric scattering in monolayer $MoS_2$ from first principles. *Phys. Rev. B* **2013**, *87*, 235312.

(40) Geim, A. K.; Grigorieva, I. V. Van der Waals heterostructures. *Nature* **2013**, *499*, 419−425.

(41) van der Zande, A. M.; Huang, P. Y.; Chenet, D. A.; Berkelbach, T. C.; You, Y.; Lee, G.-H.; Heinz, T. F.; Reichman, D. R.; Muller, D.

A.; Hone, J. C. Grains and grain boundaries in highly crystalline monolayer molybdenum disulphide. *Nat. Mater.* **2013**, *12*, 554−561.

(42) Schwierz, F. Nanoelectronics: Flat transistors get off the ground. *Nat. Nanotechnol.* **2011**, *6*, 135−136.

(43) The International Technology Roadmap for Semiconductors. 2009, http://www.itrs.net/links/2009itrs/home2009.htm.

(44) Novoselov, K. S.; Falko, V. I.; Colombo, L.; Gellert, P. R.; Schwab, M. G.; Kim, K. A roadmap for graphene. *Nature* **2012**, *490*, 192−200.

(45) Li, L.; Yu, Y.; Ye, G. J.; Ge, Q.; Ou, X.; Wu, H.; Feng, D.; Chen, X. H.; Zhang, Y. Black phosphorus field-effect transistors. *Nat. Nano* **2014**, *9*, 372−377.

(46) Kang, S. J.; Kocabas, C.; Ozel, T.; Shim, M.; Pimparkar, N.; Alam, M. A.; Rotkin, S. V.; Rogers, J. A. High-performance electronics using dense, perfectly aligned arrays of single-walled carbon nanotubes. *Nat. Nano* **2007**, *2*, 230−236.

(47) Facchetti, A. Semiconductors for organic transistors. *Mater. Today* **2007**, *10*, 28−37.

(48) S. M..Sze; Ng, K. K. *Physics of Semiconductor Devices*, 3rd ed.; Wiley-Interscience: Hoboken, NJ, 1978.